

## Magnetic energy levels of bismuth in the low-quantum-number limit\*

M. P. Vecchi<sup>†‡</sup> and M. S. Dresselhaus<sup>‡</sup>

*Department of Electrical Engineering and Center for Materials Science and Engineering, Massachusetts Institute of Technology, Cambridge, Massachusetts 02139*

(Received 15 June 1973)

A quantitative description of the electronic magnetic levels of bismuth in the low-quantum-number limit is presented. The model is based on the simplifications to the Baraff Hamiltonian made by Maltz and Dresselhaus and includes the effects of bands outside the two-band model as well as the interaction between the  $j = 0$  levels in the conduction and valence bands represented by a coupling parameter  $P$ . Magnetoreflexion results on interband Landau-level and cyclotron-resonance transitions in the low-quantum-number limit are utilized in the determination of the parameters of this model, including the first quantitative measurement of  $P$ . Values for the direct energy gap, cyclotron effective masses, and coupling parameter  $P$  are reported for  $\vec{H} \parallel$  binary and  $\vec{H} \parallel$  bisectrix axes in the temperature range  $4.2 < T < 75$  K.

### I. INTRODUCTION

The  $E(\vec{k})$  dispersion relation for the electrons at the  $L$  point in the Brillouin zone of bismuth has been studied very extensively.<sup>1-6</sup> Phenomenological models based on  $\vec{k} \cdot \vec{p}$  perturbation theory have been very successful in describing the two strongly coupled bands near the Fermi level.<sup>2,4</sup> The magnetic-energy-level structure for these coupled bands has also been studied quite extensively, and several models have been proposed.<sup>1-3,5,7</sup> The simplest of these models is the coupled two-band model of Lax,<sup>1</sup> and the most complete model available is that due to Baraff.<sup>5</sup> Of particular interest in the present work is the magnetic-energy-level structure in the regime where Landau-level spacings become large compared to the energy gap. Owing to the small energy gap and effective masses of bismuth, this regime can be achieved for magnetic fields as low as 30 kG. When Landau-level spacings are large compared with the energy gap, one expects a significant coupling between the two lowest quantum levels ( $j = 0$ ) in the conduction and valence bands. It is expected, therefore, that the magnetic-energy-level structure in the low-quantum-number limit will deviate from the simple two-band model<sup>1,2</sup> due both to the interaction with outside bands and to the interband coupling between the two  $j = 0$  levels.

Using results from magnetoreflexion experiments, Maltz and Dresselhaus<sup>7</sup> succeeded in simplifying the Baraff Hamiltonian, and the resulting model provides a very accurate description for the  $j \neq 0$  magnetic energy levels. However, due to the interband coupling of the two  $j = 0$  levels, discrepancies are to be expected in the interpretation of magnetoreflexion experiments involving the  $j = 0$  levels. In fact, the present magnetoreflexion experiments in the low-quantum-number limit reveal that the interband coupling between the two

$j = 0$  levels is an important factor at higher magnetic fields (see Sec. II).

The original work of Baraff<sup>5</sup> included a study of the coupling between the two  $j = 0$  levels, but because of their complexity, these expressions had never been applied to the interpretation of experimental results. On the basis of the present magnetoreflexion experiments in the low-quantum-number limit, it has been possible to simplify the Baraff expressions. The resulting model for the  $j = 0$  levels has been used in the interpretation of our experimental results, and all of the parameters of the model have been determined quantitatively.

Section II presents a summary of the theoretical models which have been developed in the past, emphasizing the relevant experimental evidence that motivated each model. This summary is followed by a quantitative description of the  $j = 0$  Landau levels applicable at very high magnetic fields. Section III describes the magnetoreflexion experiments that were performed to study the validity of this quantitative model throughout the temperature range  $4.2 < T < 75$  K. The unusual behavior of Landau-level transitions involving the  $j = 0$  states is utilized in the explicit determination of the various parameters which describe this model. Some concluding comments are given in Sec. IV.

### II. MAGNETIC ENERGY LEVELS OF BISMUTH

#### A. Two-band model

The energy dispersion relation for the electrons in bismuth can be approximated very accurately by considering two tightly coupled bands at the  $L$  point in the Brillouin zone. The resulting two-band model<sup>1,2</sup> follows from  $\vec{k} \cdot \vec{p}$  perturbation theory with the dispersion relation given by

$$E^{\pm}(\vec{k}) = \pm \frac{1}{2} \left( E_g^2 + 2E_g \hbar^2 \frac{\vec{k} \cdot \vec{\alpha} \cdot \vec{k}}{m} \right)^{1/2}, \quad (1)$$

where the dimensionless inverse-effective-mass tensor  $\vec{\alpha}$  is defined by

$$\vec{\alpha} = (\vec{m}^*)^{-1} = 2 \langle c | \vec{p} | v \rangle \langle v | \vec{p} | c \rangle / E_g m, \quad (2)$$

and the subscripts  $c, v$  refer to the conduction (+) and valence (-) bands separated by an energy gap  $E_g$ . The form of  $\vec{\alpha}$  can be deduced from symmetry arguments<sup>8</sup> and is shown to be given by

$$\vec{\alpha} = \begin{bmatrix} \alpha_{11} & 0 & 0 \\ 0 & \alpha_{22} & \alpha_{23} \\ 0 & \alpha_{23} & \alpha_{33} \end{bmatrix}, \quad (3)$$

where 1, 2, and 3 refer to the binary, bisectrix, and trigonal directions, respectively. The band parameters given in Eq. (1) have to be determined experimentally. The two-band model yields a nonparabolic dispersion relation with ellipsoidal constant-energy surfaces (ENP model).

Corrections to the ENP model have been considered by Cohen.<sup>4</sup> The work of Cohen included the coupling to bands outside the two-band model through the diagonal matrix elements of the secular equation. The resulting dispersion relation is nonparabolic, and the constant-energy surfaces are nonellipsoidal<sup>4,6</sup> (NENP model). Careful experiments sensitive to the shape of the Fermi surface in bismuth<sup>9</sup> show a nearly ellipsoidal constant-energy surface, and hence there seems to be no necessity for choosing the Cohen NENP model over the simpler ENP two-band model.

The experiments in bismuth which have been most informative with regard to the energy-band structure about the  $L$  point have been performed in the presence of external magnetic fields. For this reason, a great deal of attention has been given to the magnetic energy levels. The magnetic-energy-level structure derived from the ENP two-band model can be written<sup>1,2</sup>

$$E_j^{\pm}(k_z) = \pm \left[ \frac{1}{4} E_g^2 + E_g (\beta^* H j + \hbar^2 k_z^2 / 2m_c^*) \right]^{1/2}, \quad (4)$$

where  $k_z$  is the wave vector in the direction of the applied magnetic field  $H$ . In obtaining Eq. (4), it is assumed<sup>2</sup> that the spin-orbit interaction is much larger than the energy gap  $E_g$ . The magnetic energy levels as given by Eq. (4) depend on three quantum numbers: band index ( $\pm$ ), magnetic level index ( $j$ ), and wave vector ( $k_z$ ). The magnetic-energy-level structure for  $k_z = 0$  is indicated in Fig. 1.

The effective-mass tensor  $\vec{m}^*$  is related to the parameters in Eq. (4) insofar as the mass component along the magnetic field is given by

$$m_z^* = (\hat{h} \cdot \vec{m}^* \cdot \hat{h}) m, \quad (5)$$

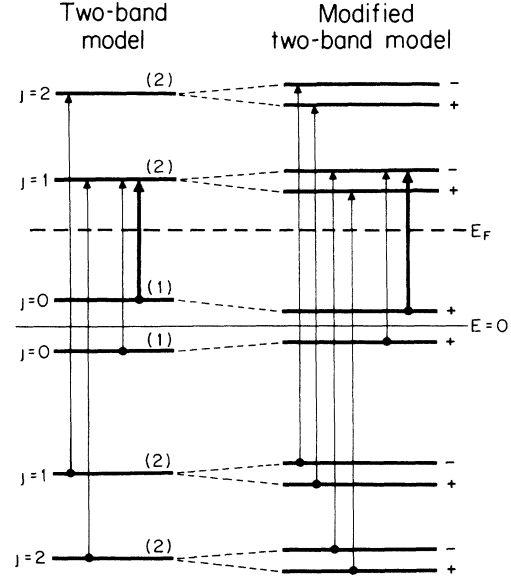


FIG. 1. Schematic representation of the magnetic energy levels of bismuth according to the strict two-band model and to the modified Baraff model. Allowed optical transitions observed in magnetoreflexion experiments are denoted by dark arrows for cyclotron-resonance transitions and by light arrows for interband Landau-level transitions. The level degeneracies for the strict two-band model are shown in parentheses. The levels of the modified two-band model are labeled by the sign of  $s$ , as in Eq. (15).

where  $\hat{h}$  is a unit vector along the magnetic field. The cyclotron effective mass  $m_c^*$  is defined by

$$m_c^* = \left( \frac{\det \vec{m}^*}{m_z^*} \right)^{1/2} m^{3/2} \quad (6)$$

and

$$\beta^* = \beta_0 \frac{m}{m_c^*}, \quad (7)$$

where  $\beta_0$  is twice the Bohr magneton,

$$\beta_0 = e \hbar / mc. \quad (8)$$

The magnetic level index  $j$  can be conveniently written in terms of the orbital and spin quantum numbers  $n$  and  $s$ :

$$j = n + \frac{1}{2} - s, \quad (9)$$

where  $n = 0, 1, 2, \dots$  and  $s = \pm \frac{1}{2}$ .

Note that in the two-band model, all Landau levels except for  $j=0$  are doubly degenerate, with the  $(n, \frac{1}{2})$  levels degenerate with the  $(n-1, -\frac{1}{2})$  levels.

#### B. Smith-Baraff-Rowell model

The magnetic energy levels of bismuth have been studied in detail by experiments that observe the

passage of or Landau levels through the Fermi surface, such as de Haas-van Alphen,<sup>10</sup> Shubnikov-de Haas,<sup>11,12</sup> magnetothermal oscillations,<sup>13</sup> and ultrasonic attenuation<sup>14</sup> studies. All of these de Haas-van Alphen-type experiments exhibit departures from the prediction of the two-band model insofar as the degeneracy of the magnetic energy levels is lifted with an observed splitting of 10–30%, depending on the magnetic field orientation.

These departures from the strict two-band model led Smith, Baraff, and Rowell<sup>11</sup> (SBR) to analyze their Shubnikov-de Haas data in terms of a modified two-band model in which the definition of a spin-mass tensor was introduced. The model used by SBR is

$$E_{n,s}^*(k_z) = \pm \left[ \frac{E_g^2}{4} + E_g \left( \beta^* H(n + \frac{1}{2}) + \frac{\hbar^2 k_z^2}{2m_s^*} - s g^* \beta_0 H \right) \right]^{1/2}, \quad (10)$$

where the effective  $g$  factor  $g^*$  is defined in terms of a spin-mass tensor  $\vec{m}_s$  by

$$(g^*)^2 = 4m^2 \frac{\hat{h} \cdot \vec{m}_s \cdot \hat{h}}{\det \vec{m}_s}. \quad (11)$$

By allowing  $\vec{m}_s$  to be different from  $\vec{m}^*$ , SBR were able to lift the degeneracy predicted by the strict two-band model and to account for the observed spin-splitting effects.

Even though the model used by SBR provides a good fit to their experimental results, there are two serious objections to its use. The first objection is the lack of a theoretical justification for the introduction of the spin mass in the form given in Eqs. (10) and (11). The second objection is that for large enough magnetic fields, the energy given by Eq. (10) for the lowest Landau level (i.e.,  $n=0$ ,  $s=\frac{1}{2}$ ) could involve the square root of a negative number, which has no physical meaning.

### C. Application to magnetoreflexion experiments

The magnetic energy levels of bismuth have also been studied by magnetoreflexion experiments.<sup>1,7,15–18</sup> These experiments observe optical transitions between Landau levels, both from the valence to the conduction band (interband) and from filled to empty levels of the conduction band (intraband or cyclotron resonance). For interband transitions, the joint density of states is singular at  $k_z=0$ , and one observes resonant transitions.<sup>7</sup> The selection rules for optical transitions at  $k_z=0$  have been determined by Wolff<sup>2</sup> and Maltz.<sup>17</sup> At the  $L$  point in the Brillouin zone the selection rules are as follows: for transitions where no  $j=0$  levels are involved,

$$\Delta j = \pm 1, \quad \Delta s = 0; \quad (12a)$$

and for transitions where the initial states are  $j=0$ , the selection rules are:

$$\Delta j = \pm 1; \quad \Delta s = \pm 1. \quad (12b)$$

For neighboring points in the Brillouin zone, these selection rules break down; nevertheless, Maltz<sup>17</sup> has shown that transitions other than those given by Eq. (12) result in broad and nonresonant magnetoreflexion structures.

Using Eq. (4) and the above selection rules, the condition for interband resonance can be written immediately as

$$\hbar\omega = |E_j^+(0) - E_{j+1}^-(0)|, \quad (13a)$$

and in terms of the band parameters as

$$\hbar\omega = (\frac{1}{4}E_g^2 + E_g\beta^*Hj)^{1/2} + [\frac{1}{4}E_g^2 + E_g\beta^*H(j+1)]^{1/2}, \quad (13b)$$

where  $\hbar\omega$  is the energy of the incident photons.

Intraband transitions are also observed by magnetoreflexion techniques. In analogy with the previous discussion, the condition for intraband optical transitions can be written

$$\hbar\omega = |E_{j+1}^+(k_z) - E_j^+(k_z)|, \quad (14a)$$

where contributions to the cyclotron-resonance line can come from a distribution of  $k_z$  values. The above equation, for the special case of  $k_z=0$ , can be expressed in terms of the band parameters as

$$\hbar\omega = [\frac{1}{4}E_g^2 + E_g\beta^*H(j+1)]^{1/2} - [\frac{1}{4}E_g^2 + E_g\beta^*Hj]^{1/2}, \quad (14b)$$

where again  $\hbar\omega$  is the energy of the incident photons.

Line-shape calculations by Maltz<sup>17</sup> provide definite guidelines for reading the experimental resonant magnetic fields for interband Landau-level transitions in bismuth. In this case, the position of the reflectivity maximum corresponds to the resonant magnetic field in Eq. (13b). Intraband transitions, on the other hand, are not restricted to  $k_z=0$  and because of the nonparabolic bands of bismuth, intraband transitions will not occur at the same photon energy for all  $k_z$  values. The line-shape analysis of Maltz<sup>17</sup> does not provide a conclusive method for the determination of the position of the  $k_z=0$  intraband transition within the experimental linewidth, because the bands outside the two-band model were found to contribute significantly to the line shape. Hence, the experimental uncertainty originating from the analysis of intraband transitions in magnetoreflexion data will be larger than from the analysis of interband resonances.

The resonant conditions for the magnetoreflexion experiment [Eqs. (13b) and (14b)] are written assuming that the two-band model applies exactly. Since it is known from de Haas-van Alphen-type experiments that there are spin-splitting effects in bismuth, one would expect that magnetoreflexion

tion traces should also show structure due to spin splittings. Detailed magnetoreflexion studies of interband Landau-level transitions by Maltz and Dresselhaus<sup>7</sup> failed to uncover any evidence for spin-splitting effects except insofar as these effects contribute to the line shape. The present work, however, establishes that magnetoreflexion resonances, in the extreme low-quantum-number limit, do in fact contain detailed information about the contribution from bands outside the two-band model to the magnetic level structure of bismuth.

#### D. Modified Baraff model

In order to be able to explain both the spin-splitting effects observed by de Haas-van Alphen-type experiments and the lack of spin-splitting effects in the magnetoreflexion experiments, it is necessary to examine the magnetic-energy-level structure of bismuth in a more rigorous fashion. In particular, the *ad hoc* model introduced by SBR, Eq. (10), fails to explain the magnetoreflexion data.

The effect of other bands on the magnetic-energy-level structure of bismuth has been studied by Baraff using perturbation-theory techniques.<sup>5</sup> The Landau-level structure for  $k_z = 0$  was developed by Baraff in terms of four undetermined tensor parameters, representing the corrections from bands outside the two-band model to the spin and orbital parts of the conduction- and valence-band wave functions. In addition, Baraff considered an interaction effect between the two  $j=0$  Landau levels which would become important when the Landau-level separation becomes comparable with  $E_g$ . In its original form, the Baraff model saw little practical utilization because of the large number of parameters that would have to be determined experimentally. By examining their magnetoreflexion results, Maltz and Dresselhaus were able to simplify the Baraff model for the  $j \neq 0$  Landau levels and they obtained the expression

$$E_{j,s}^*(0) = \pm (\frac{1}{4}E_g^2 + E_g\beta^*Hj)^{1/2} - 2s |G\beta^*|H, \quad (15)$$

where  $s = \pm \frac{1}{2}$  and  $G$  is a spin-splitting parameter, to be determined experimentally. The simplification of the Baraff model which is implied by the magnetoreflexion data is that the spin-splitting parameters of the valence and conduction bands are of  $\sim$ equal magnitude and opposite sign.

It should be emphasized that Eq. (15) includes both the orbital and spin contribution of bands outside the two-band model to first-order perturbation theory. The correction to the spin part of the wave functions appears explicitly in the parameter  $G$ , which depends on the orientation of the magnetic field. On the other hand, the corrections to the orbital part of the wave functions are included implicitly in a redefinition of  $\beta^*$ .<sup>7</sup>

Using Eq. (13a) with the selection rules given by (12a) and the expression of Eq. (15), one obtains the resonance condition for interband transitions between Landau levels with  $j \neq 0$ . It is seen that the spin terms cancel, and the resonance condition reduces precisely to the form of Eq. (13b), which was derived assuming the validity of the strict two-band model. It is possible then to understand both the spin splittings observed by de Haas-van Alphen-type experiments, and the lack of spin-splitting effects in magnetoreflexion traces involving levels with  $j \neq 0$ .

In order to study the behavior of the  $j=0$  Landau levels, it is not sufficient to consider Eq. (15) for the following reason. The two  $j=0$  Landau levels are very close to each other in energy; there is also evidence that for some magnetic field orientations, these levels move closer to each other with increasing magnetic field. It is necessary, therefore, to treat the two  $j=0$  levels in degenerate perturbation theory whenever the Landau-level separation becomes comparable to the band gap. This calculation has also been done by Baraff.<sup>5</sup> Simplification of the Baraff expression on the basis of magnetoreflexion data for both interband and intraband transitions involving the  $j=0$  levels yields the following result:

$$E_{j=0}^*(0) = \pm [(\frac{1}{2}E_g - |G\beta^*|H)^2 + P(\beta^*H)^2]^{1/2}, \quad (16)$$

where the coupling parameter  $P$  ( $P > 0$ ) in Eq. (16) is to be determined experimentally and is dependent on the orientation of the magnetic field. The magnetic-energy-level structure for the modified Baraff model is shown schematically in Fig. 1.

Of relevance to this interband coupling between the two  $j=0$  Landau levels is the cyclotron-resonance transition from the  $j=0 \rightarrow j=1$  conduction-band levels. In the present experiments, the cyclotron-resonance transition is observed for both the light binary and bisectrix electrons at much lower magnetic fields than would be predicted by either the strict two-band model of Eq. (4) or the modified two-band model of Eq. (15), which was used by Maltz and Dresselhaus in their analysis. To explain the cyclotron-resonance data, it is necessary to use the model of Eq. (16) for which the two  $j=0$  Landau levels in the low-magnetic-field regime approach each other with increasing magnetic field.

In the remaining sections of this paper, the magnetic-energy-level model given by Eqs. (15) and (16) will be used to interpret the results of magnetoreflexion experiments at several temperatures between 4.2 and 75 K. It will be seen that Eqs. (15) and (16) provide accurate quantitative descriptions of the experimental results. By using both magnetoreflexion data and information about spin splitting obtained from de Haas-van

Alphen-type data, the band parameters of bismuth are determined for the light binary and the light bisectrix electrons.

### III. MAGNETOREFLECTION EXPERIMENTS

#### A. Description of the experiment

The arrangement used for our magnetoreflexion experiments has been described in detail elsewhere<sup>18</sup> and only a few relevant features will be mentioned here. The purpose of the experiment is to measure the optical reflectivity as a function of magnetic field for several fixed incident photon energies. The experiments were carried out using the Faraday geometry, with the magnetic field parallel to the propagation vector of the light. A He-Xe gas laser was used as the photon source, providing laser lines at 7.31, 9.01, 11.3, and 18.5  $\mu$ . A low-temperature Dewar housed a superconducting magnet and provided sample temperatures from 4.2 to 75 K in magnetic fields up to 75 kG.

The bismuth samples used in this work were prepared from oriented single crystals and cut to size by a string saw. The optical face was lapped to an optical flat, and then it was mechanically polished, starting with 0.5- $\mu$  alumina grit and then with finer grits down to a size of 0.05  $\mu$ . The surface thus obtained proved to be a good mirror and no noticeable surface damage was encountered.

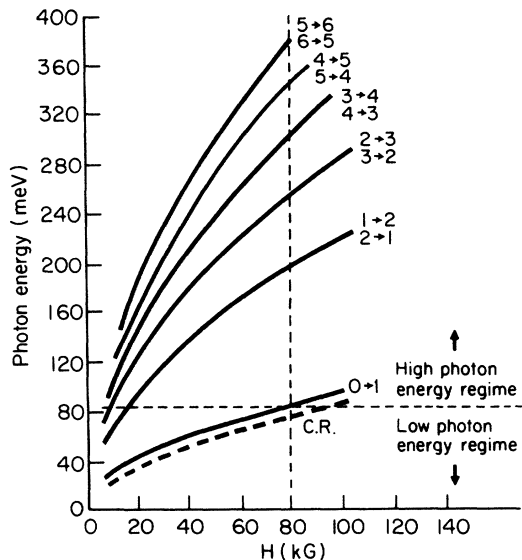


FIG. 2. Plot of the resonant magnetic fields and photon energies in the magnetoreflexion spectrum of bismuth for the light binary electrons [from Maltz and Dresselhaus (Ref. 7)]. The interband transitions are given by solid curves, the cyclotron-resonance transition by the dashed curve, and the two photon-energy regimes are indicated.

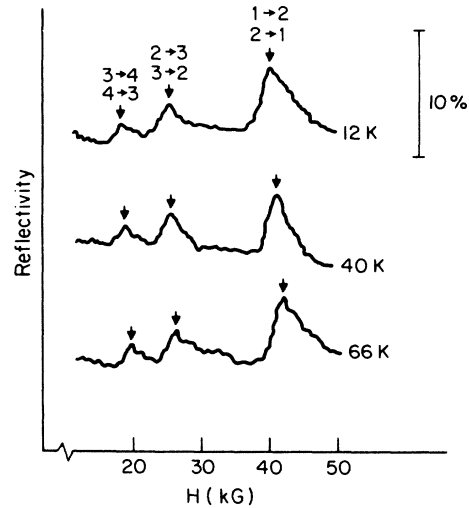


FIG. 3. Experimental magnetoreflexion traces for three different temperatures in the high-photon-energy regime. The magnetic field is along the binary direction and the photon energy is  $\hbar\omega = 137.72$  meV. The resonances are labeled in accordance with Fig. 2.

#### B. High-photon-energy results

For high magnetic fields and for  $j \neq 0$ , the resonant condition for interband transitions given by Eq. (13b) is not sensitive to the value of  $E_g$ , but only to the product  $E_g\beta^*$ . It is therefore convenient<sup>18</sup> to distinguish between the "high-" and "low-" photon-energy regimes as is illustrated in Fig. 2. In this figure, the two regimes are defined for the light binary electrons by plotting the resonant condition for interband transitions as a function of photon energy and magnetic field. The horizontal dashed line separates the high- and low-photon-energy regimes. The vertical line represents the approximate maximum magnetic field available for the present study. In Fig. 2, a transition from valence level  $j$  to conduction level  $j'$  is denoted by  $j \rightarrow j'$ .

There are two important points to consider with regard to the high-photon-energy regime. First, all the transitions involve Landau levels for which  $j \neq 0$ . This implies that the strict two-band model can be used to interpret the magnetoreflexion results (see Sec. IID). Second, the position of the resonances in the high-photon-energy regime will yield accurate values for the product  $E_g\beta^*$ , but not for  $E_g$  and  $\beta^*$  separately.

High-photon-energy data were obtained for both the light binary and light bisectrix electrons in the temperature range  $4.2 < T < 75$  K. Figure 3 shows typical experimental traces at three different temperatures for the light binary electrons. It is

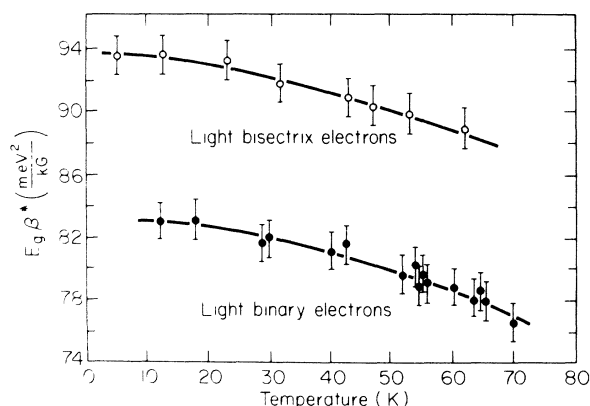


FIG. 4. Summary of the temperature dependence of  $E_g \beta^*$  deduced from the high-photon-energy results for the light binary and the light bisectrix electrons. The circles are the experimental values and the solid lines represent least-squares fits to the data.

seen that, for a fixed photon energy, the position of a given resonance moves to higher magnetic fields as the temperature increases. Since the position of the resonances is not sensitive to the value of  $E_g$  in the high-photon-energy regime, it can be concluded that the product  $E_g \beta^*$  is a function of temperature. The product  $E_g \beta^*$  is directly related to the momentum matrix elements coupling the valence and conduction bands (see Appendix). Hence, the present results establish the temperature dependence of the momentum matrix elements.

The high-photon-energy data are summarized in Fig. 4, where the product  $E_g \beta^*$  is plotted as a function of temperature for both the light binary and light bisectrix electrons. Good agreement is obtained between the values of  $E_g \beta^*$  in the present work at 4.2 K and previous results<sup>1,7,12</sup> for both magnetic field orientations. Furthermore, it is possible to compare the value of  $E_g \beta^*$  for the light binary electrons at 77 K with a previous measurement by Tichovolsky<sup>15</sup> and here, too, the agreement is excellent. The present results, however, represent the first systematic measurement of  $E_g \beta^*$  throughout the range  $4.2 < T < 75$  K, for both the light binary and light bisectrix electrons.

### C. Low-photon-energy results

Two transitions are observed in the low-photon-energy regime: the  $0 \rightarrow 1$  interband transition and the cyclotron-resonance transition.<sup>19</sup> Both of the above transitions involve  $j=0$  Landau levels; hence, it is not possible to use the strict two-band model for the interpretation of the low-photon-energy results (see Sec. IID).

The resonance condition for optical transitions involving the  $j=0$  levels results from Eqs. (15) and

(16), and is written

$$\hbar\omega = (\frac{1}{4}E_g^2 + E_g\beta^*H)^{1/2} + |G\beta^*|H \pm [(\frac{1}{2}E_g - |G\beta^*|H)^2 + P(\beta^*H)^2]^{1/2}, \quad (17)$$

where the + sign is for the  $0 \rightarrow 1$  interband transition and the - sign is for the cyclotron-resonance transition.

Magnetoreflexion traces at three different temperatures for the light binary electrons in the low-photon-energy regime are shown in Fig. 5. The temperature dependence of the band parameters is most evident from inspection of the cyclotron-resonance transitions.

The value of the spin-splitting parameter  $|G| = (6.0 \pm 1.0) \times 10^{-3}$  for the light binary electrons was calculated using data from de Haas-van Alphen-type experiments<sup>10,13</sup> and taking into consideration the magnetic field dependence of the Fermi energy.<sup>11,20</sup> Using this value of  $G$  and the values of  $E_g \beta^*$  obtained from the high-photon-energy magnetoreflexion results, the magnetoreflexion data in the low-energy regime yield values for all of the remaining parameters. These results are summarized in Figs. 6 and 7, where  $E_g$  and  $\beta^*$  are plotted as a function of temperature. The

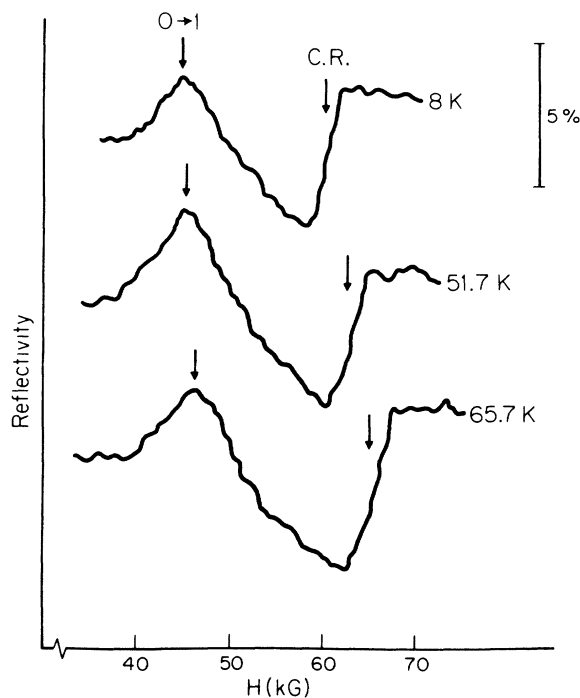


FIG. 5. Experimental magnetoreflexion traces for three different temperatures showing the cyclotron-resonance and the  $0 \rightarrow 1$  interband transitions. The magnetic field is directed along the binary direction and  $\hbar\omega = 67.00$  meV.

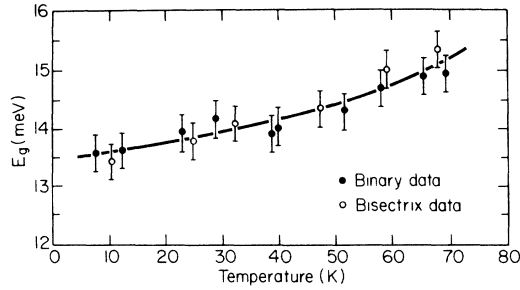


FIG. 6. Temperature dependence of the energy gap. The open circles correspond to results for  $\vec{H} \parallel$  binary and the black circles for  $\vec{H} \parallel$  bisectrix axis. The solid line represents a least-squares fit to the data.

value of the coupling parameter resulting from our data is  $P = (3.8 \pm 1.0) \times 10^{-5}$  for the light binary electrons. The magnitudes of both  $E_g$  and  $\beta^*$  presented here are in excellent agreement with recent high-frequency cyclotron-resonance experiments by Strom, Kamgar, and Koch.<sup>21</sup>

For the bisectrix electrons, no accurate determination of the spin-splitting parameters is presently available.<sup>22</sup> It was therefore necessary to use the values of  $E_g$  obtained for the light binary electrons, together with the low-photon-energy magnetoreflexion data for the light bisectrix electrons to determine a value for the spin-splitting parameter of  $|G| = (8.0 \pm 1.0) \times 10^{-3}$ . The resulting values of  $\beta^*$  for the light bisectrix electrons are shown in Fig. 7, and the coupling parameter is found to be  $P = (4.0 \pm 1.0) \times 10^{-5}$ .

It should be pointed out that both the spin-splitting parameters  $G$  and the coupling parameters  $P$  have been taken to be independent of temperature. The experimental uncertainty is such that it is not possible to resolve a temperature dependence for either of these perturbation parameters.

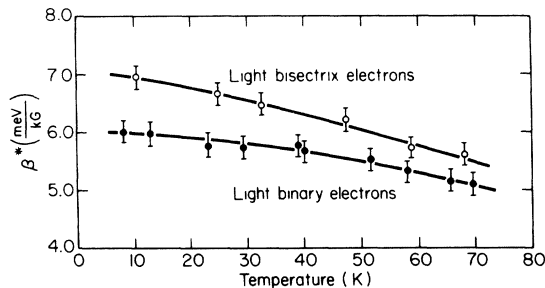


FIG. 7. Temperature dependence of  $\beta^*$  for the light binary and the light bisectrix electrons. The circles are the experimental values, and the solid lines represent least-squares fits to the data.

The general behavior of the magnetic-energy-level structure as given by Eqs. (15) and (16) is shown in Fig. 8. This figure is a plot of the energy for each Landau level at  $k_z = 0$  as a function of magnetic field, using the band parameters for the light binary electrons obtained from our experiments at  $T = 4.2$  K. Contrary to the behavior of all other Landau levels, it is seen that the  $j = 0$  levels are not monotonic functions of magnetic field. In particular, at low magnetic fields, the conduction- and valence-band  $j = 0$  levels move towards each other, but as the interband coupling effect becomes significant, the two  $j = 0$  levels repel each other. The magnetic field value for minimum separation is  $\sim 100$  kG for the light binary electrons. A similar analysis yields a magnetic field value for minimum separation of  $\sim 80$  kG for the light bisectrix electrons.

#### IV. CONCLUDING REMARKS

The magnetic-energy-level structure described by Eqs. (15) and (16) has been shown to be con-

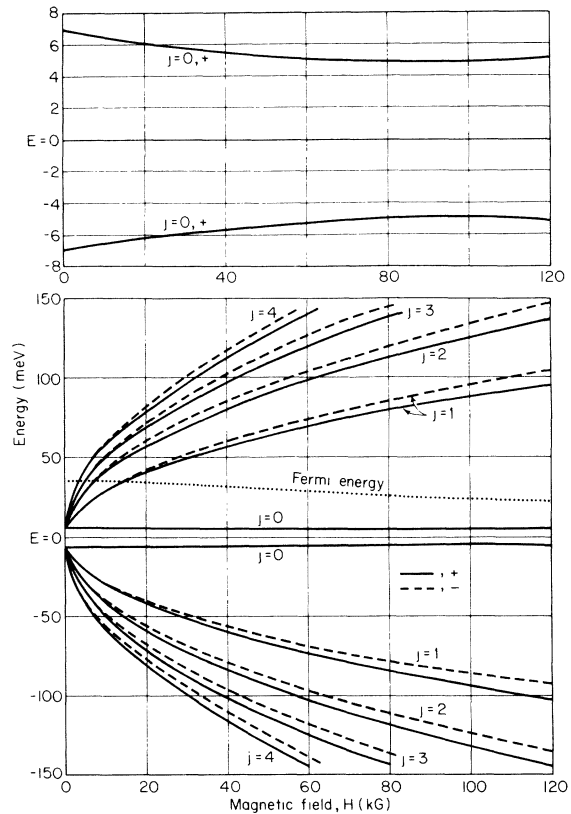


FIG. 8. Plot of the positions of the Landau-level extrema for the light binary electrons at  $T \sim 4.2$  K. The expanded scale shows the behavior of the  $j = 0$  levels in detail. The curves were drawn using Eqs. (15) and (16) with the band parameters presented in the text. The + and - signs refer to the sign of  $s$  as given in Eq. (15).

sistent with available experimental magnetoreflexion and de Haas-van Alphen-type results. The algebraic expressions are rather simple in form, and all of the necessary parameters have been determined for both the light binary and the light bisectrix electrons. From a practical point of view, the question arises as to the magnetic field ranges in which the various corrections to the two-band model become important. For the  $j \neq 0$  levels, the spin-splitting term represented by the parameter  $G$  is found to be  $\leq 10\%$  of the Landau-level separation, for both the light binary and light bisectrix electrons. Therefore spin-splitting effects are important only for high-resolution studies of the magnetic-energy-level structure of bismuth.

For the  $j=0$  levels, the spin-splitting correction is of the same magnitude as for the  $j \neq 0$  Landau levels. However, the interband coupling between the two  $j=0$  levels, represented by the parameter  $P$  in Eq. (16), becomes the dominant factor at magnetic fields such that  $(\frac{1}{2}E_g - G\beta^*H)^2 \leq P(\beta^*H)^2$ . This condition corresponds to  $H \geq 90$  kG for the light binary electrons, and to  $H \geq 70$  kG for the light bisectrix electrons.

The magnetic field dependence of the  $j=0$  level of the conduction band has also been deduced from Alfvén-wave transmission experiments by Takano and Kawamura.<sup>23</sup> While the results of the present paper are in good agreement with the work of Takano and Kawamura at low magnetic fields, there are discrepancies between the two investigations at higher magnetic fields. These differences can be attributed to the neglect by these authors of the coupling between the two  $j=0$  Landau levels which our experiments show to be important at high magnetic fields. Further work is now in progress to extend our magnetoreflexion studies to even higher magnetic fields where the effect of the coupling between the two  $j=0$  levels will be larger and therefore greater sensitivity to the parameter  $P$  will be achieved.

The present magnetoreflexion experiments in the range  $4.2 < T < 75$  K also provided a measurement of the temperature dependence of the band parameters. Of particular interest is the observa-

tion of a temperature dependence of the momentum matrix elements. Work is currently in progress to relate the above temperature dependences to the energy-band structure about the  $L$  point, and will be reported elsewhere.

#### ACKNOWLEDGMENTS

We are grateful to Dr. C. R. Hewes and D. A. Platts for their help with the experiments and for many useful discussions. We would also like to thank E. J. Alexander for supplying and preparing the bismuth crystals used for this work. Thanks are also due to Dr. G. F. Dresselhaus, Professor D. Shoenberg, and Professor H. Kawamura for helpful discussions. Finally, we acknowledge the help of Dr. J. R. Pereira in calculating the magnetic field dependence of the Fermi energy.

#### APPENDIX: RELATION BETWEEN $E_g\beta^*$ AND THE MOMENTUM MATRIX ELEMENTS

We present here explicit expressions for the product  $E_g\beta^*$  for  $H$  along the binary and bisectrix directions in terms of the appropriate components of the momentum matrix elements.

The components of the square of the momentum matrix elements coupling the conduction and valence bands are defined by

$$P_{ij}^2 = \langle c | p_i | v \rangle \langle v | p_j | c \rangle. \quad (18)$$

Using the notation of Eq. (2), one then obtains the relation

$$P_{ij}^2 = \frac{1}{2}E_g m \alpha_{ij}. \quad (19)$$

For the light binary electrons, the unit vector in the direction of the applied magnetic field is given by  $\hat{h} = (-\frac{1}{2}, \pm \frac{1}{2}\sqrt{3}, 0)$ , where the  $+$ ,  $-$  signs correspond to the two equivalent ellipsoids. Using Eqs. (5)–(7) and (19), one obtains<sup>18</sup>

$$(E_g\beta^*)_{bn} = (\beta_0/m)(P_{22}^2 P_{33}^2 + 3P_{11}^2 P_{33}^2 - P_{23}^4)^{1/2}. \quad (20)$$

The corresponding result for the light bisectrix electrons is obtained using  $\hat{h} = (0, 1, 0)$  to yield<sup>18</sup>

$$(E_g\beta^*)_{bx} = 2(\beta_0/m)(P_{11}^2 P_{33}^2)^{1/2}. \quad (21)$$

\*Work supported by the Advanced Research Projects Agency and by the National Science Foundation.

†Instituto Venezolano de Investigaciones Científicas (IVIC) predoctoral Fellow.

‡Visiting Scientist, Francis Bitter National Magnet Laboratory, Massachusetts Institute of Technology, Cambridge, Mass., supported by the National Science Foundation.

<sup>1</sup>R. N. Brown, J. G. Mavroides, and B. Lax, *Phys. Rev.* **129**, 2055 (1963).

<sup>2</sup>P. A. Wolff, *J. Phys. Chem. Solids* **25**, 1057 (1964).

<sup>3</sup>M. H. Cohen and E. I. Blount, *Philos. Mag.* **5**, 115

(1960).

<sup>4</sup>M. H. Cohen, *Phys. Rev.* **121**, 387 (1961).

<sup>5</sup>G. A. Baraff, *Phys. Rev.* **137**, A842 (1965).

<sup>6</sup>M. S. Dresselhaus, in *Proceedings of the Conference on the Physics of Semimetals and Narrow Gap Semiconductors*, edited by D. L. Carter and R. T. Bate (Pergamon, New York, 1970), p. 3.

<sup>7</sup>M. Maltz and M. S. Dresselhaus, *Phys. Rev. B* **2**, 2877 (1970).

<sup>8</sup>S. Golin, *Phys. Rev.* **166**, 643 (1968); L. M. Falicov and S. Golin, *Phys. Rev.* **137**, A871 (1965).

<sup>9</sup>R. N. Bhargava, *Phys. Rev.* **156**, 785 (1967).



- <sup>10</sup>J. S. Dhillon and D. Shoenberg, *Philos. Trans. R. Soc. Lond., A* **248**, 1 (1955); Y. Saito, *J. Phys. Soc. Jap.* **18**, 1845 (1963).
- <sup>11</sup>G. E. Smith, G. A. Baraff, and J. M. Rowell, *Phys. Rev.* **135**, A 1118 (1964).
- <sup>12</sup>H. T. Chu and Y. Kao, *Phys. Rev. B* **1**, 2369 (1970).
- <sup>13</sup>B. McCombe and G. Seidel, *Phys. Rev.* **155**, 633 (1966).
- <sup>14</sup>K. Tayoda, Y. Sawada, and H. Kawamura, *J. Phys. Soc. Jap.* **32**, 653 (1972).
- <sup>15</sup>E. J. Tichovolsky, SM thesis (MIT 1969) (unpublished).
- <sup>16</sup>E. J. Tichovolsky and J. G. Mavroides, *Solid State Commun.* **7**, 927 (1969).
- <sup>17</sup>M. Maltz, Ph. D. thesis (MIT 1968) (unpublished).
- <sup>18</sup>M. P. Vecchi, SM thesis (MIT 1972) (unpublished).
- <sup>19</sup>For the available range of photon energies and magnetic fields, the only cyclotron-resonance transition which is observed is from the  $j=0 \rightarrow j=1$  conduction-band levels.
- <sup>20</sup>J. R. Pereira (private communication).
- <sup>21</sup>U. Strom, A. Kamgar, and J. F. Koch, *Phys. Rev. B* **7**, 2435 (1973).
- <sup>22</sup>J. E. Kunzler and F. S. L. Hsu, in *The Fermi Surface*, edited by W. A. Harrison and M. B. Webb (Wiley, New York, 1960), p. 88.
- <sup>23</sup>S. Takano and H. Kawamura, *J. Phys. Soc. Jap.* **28**, 348 (1970).